CELL CYCLE
2019, VOL. 18, NO. 12, 1407–1421
https://doi.org/10.1080/15384101.2019.1618126

Taylor & Francis
Taylor & Francis Group

RESEARCH PAPER

OPEN ACCESS Check for updates

Aurora kinase B-phosphorylated HP1α functions in chromosomal instability

Monique M. Williams[a], Angela J. Mathison [b,c], Trent Christensen[a], Patricia T. Greipp[d], Darlene L. Knutson[d], Eric W. Klee[a], Michael T. Zimmermann [e,f], Juan Iovanna [g], Gwen A. Lomberk [b,c,h], and Raul A. Urrutia[b,c,i]

[a]Departments of Biochemistry and Biostatistics, Mayo Clinic, Rochester, MN, USA; [b]Genomics and Precision Medicine Center (GSPMC), Medical College of Wisconsin, Milwaukee, WI, USA; [c]Division of Research, Department of Surgery, Medical College of Wisconsin, Milwaukee, WI, USA; [d]Medical Genome Facility, Cytogenetics Core Laboratory, Rochester, MN, USA; [e]Bioinformatics Research and Development Laboratory, Genomics Sciences and Precision Medicine Center, Medical College of Wisconsin, Milwaukee, WI, USA; [f]Clinical and Translational Sciences Institute, Medical College of Wisconsin, Milwaukee, WI, USA; [g]Centre de Recherche en Cancérologie de Marseille (CRCM), INSERM U1068, CNRS UMR 7258, Aix-Marseille Université and Institut Paoli-Calmettes, Parc Scientifique et Technologique de Luminy, Marseille, France; [h]Department of Pharmacology and Toxicology, Medical College of Wisconsin, Milwaukee, WI, USA; [i]Department of Biochemistry, Medical College of Wisconsin, Milwaukee, WI, USA

ABSTRACT

Heterochromatin Protein 1 α (HP1α) associates with members of the chromosome passenger complex (CPC) during mitosis, at centromeres where it is required for full Aurora Kinase B (AURKB) activity. Conversely, recent reports have identified AURKB as the major kinase responsible for phosphorylation of HP1α at Serine 92 (S92) during mitosis. Thus, the current study was designed to better understand the functional role of this posttranslationally modified form of HP1α. We find that S92-phosphorylated HP1α is generated in cells at early prophase, localizes to centromeres, and associates with regulators of chromosome stability, such as Inner Centromere Protein, INCENP. In mouse embryonic fibroblasts, HP1α knockout alone or reconstituted with a non-phosphorylatable (S92A) HP1α mutant results in mitotic chromosomal instability characterized by the formation of anaphase/telophase chromatin bridges and micronuclei. These effects are rescued by exogenous expression of wild type HP1α or a phosphomimetic (S92D) variant. Thus, the results from the current study extend our knowledge of the role of HP1α in chromosomal stability during mitosis.

ARTICLE HISTORY
Received 20 March 2019
Revised 17 April 2019
Accepted 8 May 2019

KEYWORDS
HP1α; CBX5; Aurora Kinase; chromosomal instability

Introduction

Members of the Heterochromatin Protein 1 (HP1) family of conserved non-histone chromatin proteins, first discovered in *Drosophila melanogaster*, were originally noted for their role in heterochromatin-mediated gene silencing [1,2]. These proteins have two well-characterized functional domains: an amino-terminal chromodomain (CD) and a carboxyl-terminal chromo shadow domain (CSD) – as well as a flexible linker that connects them [3,4]. Mammalian genomes encode three HP1 proteins; HP1α (CBX5), HP1β (CBX1), and HP1γ (CBX3). These proteins work as epigenetic regulators and readers of the histone 3 lysine 9 dimethyl (H3K9me2) and trimethyl (H3K9me3) marks [5,6]. H3K9me2 is deposited by the histone methyltransferases EHMT1 (GLP) or EHMT2 (G9a), while H3K9me3 is deposited by SUV39H1 or SUV39H2. These marks are then bound by HP1 proteins to form heterochromatin and cause transcriptional repression [7,8]. Multiple studies have demonstrated a role for HP1 proteins in epigenetic gene silencing, chromatin modification, DNA replication and repair, nuclear architecture, and chromatin stability [5,9–12]. However, how these proteins are regulated by membrane-to-nuclear signaling cascades in order to participate in these functions remains a matter of active investigation.

Previous studies investigating the function of HP1α during mitosis have shown that it associates with members of the chromosome passenger complex (CPC), localizing HP1α to the centromere [13]. The CPC is composed of four proteins Borealin (CDCA8), Survivin (BIRC5), Inner Centromere Protein (INCENP), and Aurora Kinase B (AURKB). These are all necessary for coordinating and regulating critical mitotic events, from chromosome condensation at the beginning of mitosis to

CONTACT Raul A. Urrutia glomberk@mcw.edu; Gwen A. Lomberk, glomberk@mcw.edu
Supplemental data for this article can be accessed here.

cytokinesis at the end [14,15]. Association of HP1α with the CPC is mediated through its chromoshadow domain and its specific binding with Borealin [16,17] and INCENP [13,18,19], but independent of the chromatin reading function of HP1α [20,21]. The interaction of HP1α with components of the CPC is thought to promote its recruitment to the centromeres after the initial ejection of this reader protein from chromatin at prophase [6,10,18,22,23]. Furthermore, its association with the CPC is required for full Aurora Kinase B (AURKB) activity [18]. More recently, it has been published that AURKB, which is overexpressed in several tumor types and associated with poor prognosis in cancer patients, is the major mitotic kinase that phosphorylates HP1α at Serine 92 [24], which is in agreement with observations in our laboratory.

In this study, we extend investigations on the role of HP1α as an effector of mitotic kinase pathways and demonstrate that this AURKB-modified target localizes to the centromere-kinetochore complex. This suggests a role in maintaining mitotic fidelity. We find that loss of HP1α leads to chromosomal instability, which is dependent on its AURKB-mediated phosphorylation. This knowledge underscores the importance of chromatin proteins as mediators of chromosomal stability downstream of pro-oncogenic pathways, such as AURKB.

Materials and methods

Cell culture and synchronization

HeLa human cervical adenocarcinoma cells were cultured according to the American Type Culture Collection (ATCC) guidelines. For synchronization studies, HeLa cells were arrested in G1/S by double thymidine block as previously described [25]. Briefly, cells were plated at 80% confluence, allowed to attach, and then incubated in 2mM thymidine (Millipore) for 18hr. Cells were washed once with Phosphate Buffered Saline (PBS, 1.37 M NaCl, 27 mM KCl, 100mM Na_2HPO_4, 18mM KH_2PO_4) and released with normal growth medium for 9 hr. For a second arrest, 2mM thymidine was added to the cells for 17hr. Cells were washed once with PBS and lysates were collected at the indicated time points post-release for Western blotting or fixed at 6, 8, and 9hr for immunofluorescence.

Pharmacological inhibition and siRNA knockdown of AURKB

HeLa cells were arrested in mitosis by treatment with nocodazole (2μg/ml, Sigma-Aldrich) for 16hr or 1μM S-trityl-L-cysteine (STLC) for 17 hr followed by a 1 hr incubation with 200nM hesperadin (Selleckchem) to inhibit AURKB activity and 10μM of the proteasome inhibitor MG132 (Sigma-Aldrich) to avoid mitotic exit [26]. AURKB was knocked down in HeLa cells by transient transfection with a siRNA smartpool (siAURKB or scrambled control, siCTRL) according to manufacturer's protocols (Dharmacon Inc). Cells were then fixed for immunofluorescence and PLA or lysed for Western blotting.

Western blotting

Proteins were isolated from cells either by lysis in RIPA (20 mM Tris-HCl (pH 7.5) 150 mM NaCl, 1 mM Na_2EDTA 1 mM EGTA 1% NP-40 1% sodium deoxycholate), supplied with protease and phosphatase inhibitor cocktails (Thermo Fisher Scientific) for 20 min on ice or in 4X Laemmli Buffer (250mM Tris pH 6.8, 20% glycerol, 8% SDS, 0.0025% bromophenol blue, 1mM β-mercaptoethanol). Western blotting was performed as previously described [27]. Membranes were blocked in either 3% BSA or 5% milk for 1 hr prior to probing with primary antibodies overnight at 4°C with rocking. The primary antibodies incubated in 3% BSA are as follows: HP1α (1:1000, Cell Signaling Technology), P-S92-HP1α (1:2000, Abcam), P-S10-Histone 3 (P-S10-H3, 1:5000, Millipore), AURKB (1:1000, Cell Signaling Technology), anti-Cyclin B1 (CCNB1, 1:1000, Abcam), and anti-INCENP (Millipore). The primary antibodies incubated in 5% milk are as follows: β-actin (ACTB, 1:5000, Sigma-Aldrich), His (1:5000, Omni D-8, Santa Cruz Biotechnology), and anti-INCENP (Millipore). Anti-mouse or anti-rabbit secondary antibodies (1:5000, Millipore) were incubated on the membranes for 1 hr at room temperature with shaking, followed by detection of bands with chemiluminescence (Thermo Fisher Scientific). Quantification of bands in n = 3 experiments was done using ImageJ [28] with statistical significance determined by Student's t-tests in GraphPad Prism 7.

Immunofluorescence (IF) and confocal microscopy

HeLa cells were plated on poly-L-lysine coated circular coverslips (0.1mg/ml poly-L-lysine) and allowed to adhere for 6 hr prior to the start of the double thymidine synchronization protocol. Cells were fixed at the desired time points with 4% formaldehyde, permeabilized with 0.2% Triton-X 100 and blocked with CAS-Block (Invitrogen) for 30 min at 37°C. Double immunofluorescence staining was performed by co-incubating cells with anti-HP1α (1:200, Cell Signaling) or anti-P-S92-HP1α (1:50, Abcam) and anti-Aurora B (1:50, Abcam), anti-INCENP (1:200, Thermo Fisher Scientific), or anti-CENPA (1:100, Abcam) primary antibodies. Alexa Fluor 488 and Alexa Fluor 555 secondary antibodies (Invitrogen) corresponding to the primary antibody species were added (1:500 and 1:250, respectively) for fluorescent detection of the proteins. Coverslips were mounted in VectaShield mounting media with DAPI (Vector Laboratories) for confocal microscopy. Control and experimental *Cbx5* fl/fl CAGGCre-ER MEFs were plated on rat tail collagen I coated coverslips (10μg/ml, Sigma-Aldrich), allowed to attach for 6 hr, and then treated with 4-Hydroxytamoxifen (4□-OHT, Sigma-Aldrich) with or without adenovirus transduction (EV, WT HP1α, S92A-HP1α, or S92D-HP1α) at 200 MOI. Immunofluorescence staining with anti-HP1α was performed as described above or anti-His (Omni D-8, Santa Cruz Biotechnology). Coverslips were mounted in ProLong Gold Antifade mounting media (with DAPI, Invitrogen). All images were acquired using 40x and 100x oil objective lenses on a Zeiss LSM 780 confocal microscope. Colocalization was calculated with the Manders overlap coefficient (MOC) in a total of 150 cells from three independent experiments [29,30]. Statistical significance was assessed with Student's t-test in GraphPad Prism 7.

Proximity ligation assay (PLA)

HeLa cells were plated on poly-L-lysine coated circular coverslips (0.1mg/ml poly-L-lysine) and allowed to adhere overnight prior to transfection with control or AURKB-targeting siRNA (siAURKB, Dharmacon). Cells were treated with 1 μM S-trityl-L-cysteine (STLC), a specific inhibitor of human mitotic kinesin Eg5 [31,32], for 18 hr to enrich the mitotic population. HeLa cells were also treated with STLC in combination with MG132 and hesperadin to enrich the mitotic population and inhibit the kinase activity of AURKB. The cells were subsequently subjected to co-staining with anti-P-S92-HP1α (1:50, Abcam) and anti-Aurora B (1:50, Abcam) or anti-INCENP (1:200, Thermo Fisher Scientific). Proximity ligation was performed using the DuoLink® PLA kit according to the manufacturer's instructions (Sigma-Aldrich). The PLA experiments are quantified by counting the number of dots per cell in 150 cells, n = 3 independent experiments. Statistical significance was assessed with Student's t-test in GraphPad Prism 7.

Immunoprecipitation (IP) and mass spectrometry

Immunoprecipitation of HP1α was performed by conjugating the HP1α antibody (Abcam, ab77256) or control IgG antibody to Protein A/G Magnetic Beads (ThermoFisher Scientific) through disuccinimidyl suberate (DSS) crosslinking. HeLa cells were synchronized with double thymidine block and released for 9 hr, corresponding to cells in mitosis [27]. Cells were lysed with IP Lysis/Wash Buffer (Thermo Scientific-Pierce), and lysates were incubated overnight with the antibody conjugates at 4°C. Immunoprecipitated complexes were washed, eluted and run on a 4–15% Criterion™ Tris-HCl Protein Gel (Bio-Rad). The gel was subsequently visualized with BioSafe™ Coomassie Stain (Bio-Rad). Each gel lane was divided into eight sections, de-stained, dehydrated, dried, and subjected to trypsin digestion. Subsequently, liquid chromatography (LC)-ESI-MS/MS analysis was performed on a Thermo Scientific LTQ Orbitrap mass spectrometer at the Mayo Clinic Proteomics Core.

Generation of *Cbx5* fl/fl CAGGCRe-ER mice

All animal protocols incorporated guidelines outlined in the Guide for Care and Use of Laboratory Animals from the National Institutes of Health as per Mayo Clinic requirements. Experiments were performed under the protocol (A24415) as reviewed and approved by Mayo Clinic's

Institutional Animal Care and Use Committee (IACUC), Rochester, MN.

Cbx5 (Cbx5tm1a(EUCOMM)Wtsi) mice were re-derived at the European Mouse Mutant Archive from embryotic stem cells generated by the Wellcome Trust Sanger Institute (ESC clone ID: EPD0445_4_A07). Mice were backcrossed with FLP (129S4/SvJaeSor-Gt(ROSA)26Sortm1(FLP1) Dym/J, Jackson Laboratory, Catalog 003946) to remove neomycin cassette and C57Bl/6 mice for greater than 10 generations. To generate tamoxifen inducible deletion of the *Cbx5* gene, mice were crossed with CAGGCre-ER lines with Cre expression driven from the chicken beta-actin promoter and cytomegalovirus (CMV) enhancer (B6.Cg-Tg (CAG-cre/Esr1*)5Amc/J, Jackson Laboratory, Catalog 004682). Mice were bred to homozygousity for the floxed exon 3 of *Cbx5* and heterozygous for CAGGCre-ER.

Cbx5 fl/fl CAGGCRe-ER mouse embryonic fibroblast isolation and gene knockout

Mouse embryotic fibroblasts (MEFs) were prepared as previously described [33]. Briefly, at embryotic day 13, pregnant females were sacrificed, and embryos removed to sterile tissue culture conditions. All embryos were processed separately and genotyped to identify control *Cbx5* fl/fl CAGGCre-ER- and experimental *Cbx5* fl/fl CAGGCre-ER+ MEFs. Embryos were disrupted by mechanical and chemical methods (TrypLE Express, ThermoFisher Scientific). Cells were allowed to attach overnight in complete growth media (DMEM +10%FBS +Antibiotic/Antimycotic +L-glutamine). MEFs were cultured for approximately one week before cryopreservation of the lines. Additionally, small batches of MEFs were immortalized (*iCbx5*) by incubation with ecotropic retrovirus containing SV40 large T antigen (EcoPack2-293; Clontech) as previously described [34].

At passage 2 primary and immortalized, control and experimental MEFs were plated to 75% confluence, allowed to attach overnight, and then serum starved for 24hr prior to treatment with 50nM 4′-OHT for 48hr. After 48hr, cells were returned to complete medium (containing 10% FBS). Hereafter, control and experimental MEFs are designated only by their presence or absence of Cbx5, respectively, *Cbx5* fl/fl CAGGCre-ER- (*Cbx5* +/+) and *Cbx5* fl/fl CAGGCre-ER+ (*Cbx5* -/-). To rescue *Cbx5* expression, MEFs upon serum starvation were concomitantly transduced with adenovirus (empty vector (EV), wild type HP1α (WT), S92A-HP1α, or S92D-HP1α) at 200 MOI. The cells were then fixed for immunofluorescence staining or collected at 0, 24, 48hr in 4X Laemmli Buffer for western blot.

Fluorescent in situ hybridization (FISH)

Primary and immortalized, control and experimental *Cbx5* MEFs (*Cbx5* +/+, *Cbx5* -/-, *iCbx5* +/+, *iCbx5* -/-, respectively) were submitted to the Mayo Clinic Cytogenetics Core Facility for FISH analysis with a Pan-centromeric probe (Cambio Ltd). Briefly, cells were split to 50% confluence, incubated overnight, and then treated with colcemid (0.1μg/ml, KaryoMax Gibco) for 4 hr at 37°C. Mitotic cells were harvested, washed, swollen in a hypotonic solution (0.075 M KCl, 37°C), and fixed with methanol: glacial acetic acid (3:1). Twenty metaphase spreads were prepared from cells in each experimental condition and pan-centromeric probe FISH performed according to the manufacturer's instructions (Cambio Ltd). Images were captured and analyzed using the Applied Imaging CytoVision™ Karyotyping System (Leica Biosystems). Chromosomal abnormalities were counted in 60 spreads from three independent experiments and statistical significance assessed with a Student's t-test in GraphPad Prism 7.

Adenovirus production for overexpression of HP1α and mutants

For the production of recombinant adenovirus, His/HP1α cDNA was subcloned from pcDNA 3.1/HisC (Invitrogen) and inserted into the pacAd5-CMV -K-N pA backbone. The HP1α-S92A and HP1α-S92D mutants were generated via the QuikChange II XL Site-Directed Mutagenesis Kit (Agilent Technologies) utilizing synthesized primers (Supplementary Table 1) (Integrated DNA Technologies) and verified via sequencing (Mayo Clinic Sequencing Core). Empty vector (EV), wild type (WT), and mutant plasmids were packaged into adenoviral particles and viral titer determined by the Viral Vector Core at the University of Iowa.

Chromatin bridges and micronuclei were quantified in greater than 500 cells over three independent imaging experiments and statistical significance determined by a Student's t-test in GraphPad Prism 7.

Results

Phosphorylated HP1α co-localizes to centromere-kinetochore domains during mitosis

Recent studies have shown that AURKB phosphorylates HP1α during mitosis [18,24]. To further explore the role of this mitotic-specific phosphorylation event, we performed time course analysis of synchronized HeLa cells. We first used double thymidine block followed by release to collect lysates through the cell cycle and perform Western blots, which confirmed that S92 HP1α phosphorylation peaks during mitosis (8 to 10 hr time points) while total β-actin (ACTB) protein levels remained constant (Supplementary Figure 1A, Supplementary Figure 2, full blots). This increased phosphorylation coincided with higher levels of AURKB and two other known mitosis markers, P-S10-H3 and Cyclin B1 (CCNB1), at the same time points. Confocal microscopy of these cells also demonstrated that, in contrast to total HP1α protein (Supplementary Figure 1B), S92-phosphorylated HP1α is absent from interphase cells and becomes detectable at the beginning of prophase, persisting until telophase (Supplementary Figure 1C). However, the functional role of this posttranslational modification in cell division remains to be fully defined. Consequently, we performed immunofluorescence experiments which show that S92-phosphorylated HP1α concentrates at the centromere-kinetochore domains as early as prometaphase and colocalizes with AURKB (Figure 1(a)) and another chromosome passenger complex member, INCENP, at metaphase (Figure 1(b)). Next, using immunoprecipitation of total HP1α both unphosphorylated and phosphorylated populations of this protein, from lysates of HeLa cells arrested in mitosis followed by mass spectrometry analysis, we confirmed the specificity of HP1α binding to INCENP and other centromere-kinetochore components (Table 1). These results are congruent with additional findings that P-S92-HP1α also localizes near CENPA (Figure 1(c)), the histone variant that is incorporated into mitotic centromeres in place of histone H3 [35–37]. High-resolution imaging of the overlay (insets, Figure 1(a,b)) demonstrated that P-S92-HP1α has significant co-localization with AURKB and INCENP, both located in centromeric heterochromatin [38]. Notably, however, P-S92-HP1α was located in close proximity but distinctly not colocalizing with CENPA (insets, Figure 1(c)), which likely reflects that this modified form of HP1α is not binding directly to CENPA-containing nucleosomes of the inner kinetochore [38]. Combined, these results demonstrate that P-S92-HP1α co-localizes with key proteins responsible for the proper formation of centromeric heterochromatin during mitosis.

Disruption of Aurora B function eliminates pool of P-S92-Hp1α at centromeric heterochromatin

Since HP1α has been associated with full activation of AURKB [18], we sought to investigate the impact of AURKB activation on HP1α. We subsequently studied the localization P-S92-HP1α upon pharmacological inhibition of AURKB activity with hesperadin (Figure 2(a,b)). P-S92-HP1α colocalization with AURKB at centromere-kinetochore domains was completely lost in +hesperadin cells, as measured by a Manders overlap coefficient (MOC) [29,30] (0 ± 0 MOC +hesperadin compared to 0.66 ± 0.07 MOC control cells-hesperadin, $p < 0.001$). Colocalization with INCENP at the same region (Figure 2(c,d)) was also significantly reduced in +hesperadin cells (0.43 ± 0.05 MOC +hesperadin compared to 0.92 ± 0.03 MOC control cells-hesperadin, $p < 0.01$). Activity of hesperadin on AURKB was confirmed by Western blot (Figure 2(e); Supplementary Figure 3A) in that P-S10-H3 (phosphorylation of histone 3, serine 10) is active in the presence of nocodazole, but markedly reduced upon addition of hesperadin. While we found a reduction in the level of P-S92-HP1α upon hesperadin treatment, levels of total HP1α did not change (Figure 2(e); Supplementary Figure 3A, 3B). Notably, localization of the non-chromatin-associated cytoplasmic pool of phosphorylated HP1α was not affected by the absence or inhibition of AURKB (Figure 2(a,c)), suggesting that another kinase may also phosphorylate HP1α at S92 and cooperate with

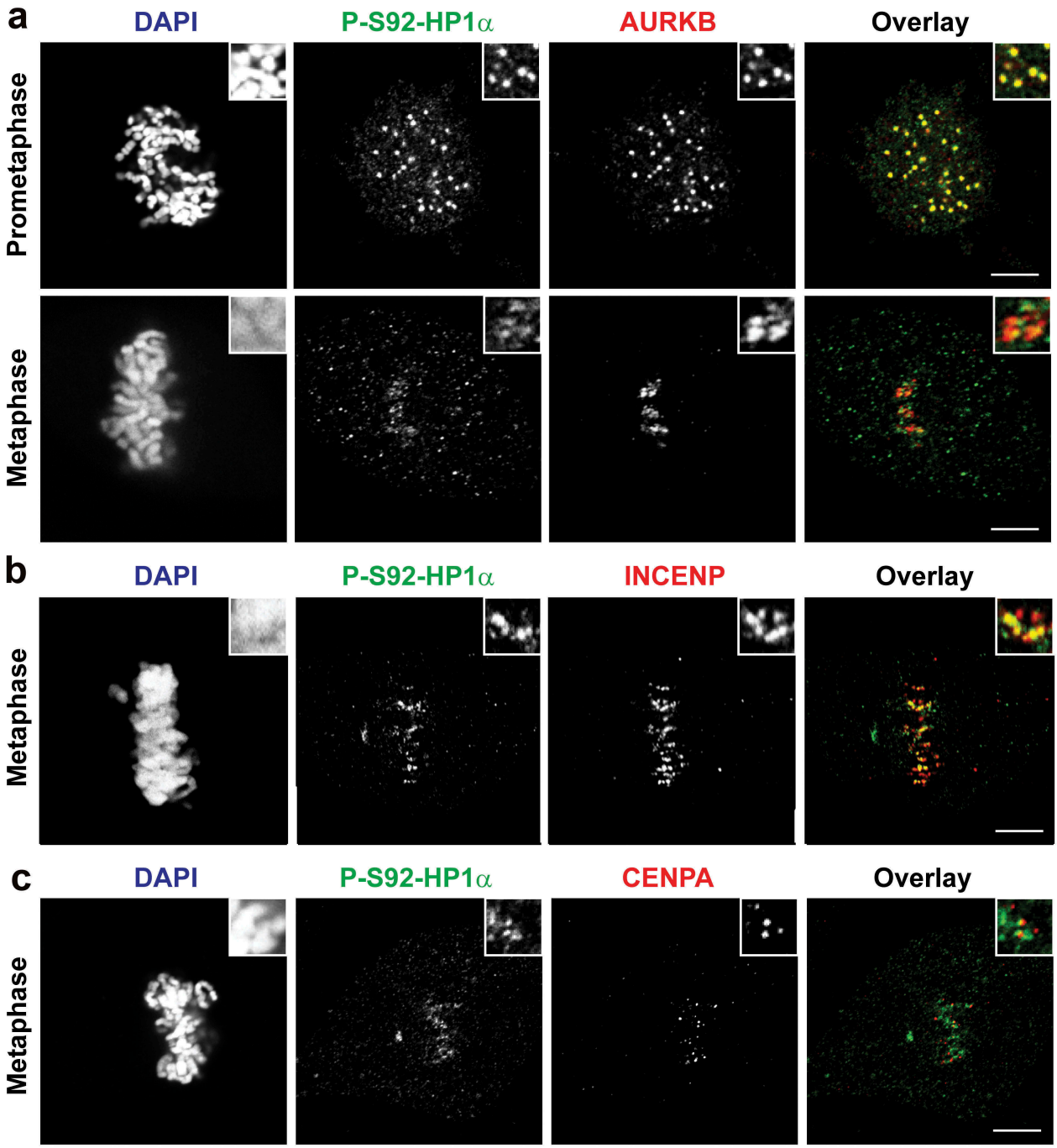

Figure 1. S92-Phosphorylated HP1α localizes to the centromere in mitosis. Representative images of immunofluorescence of the colocalization of P-S92-HP1α with three centromere markers, AURKB (Aurora Kinase B), INCENP (Inner centromere protein), and CENPA (Centromere protein A). HeLa cells were synchronized via double thymidine block and fixed at 9 hr post-release from the second block which corresponds with the mitotic cell population. Overlays are shown on far-right panel with magnified insert. (a) Colocalization of P-S92-HP1α (green) and AURKB (red) at prometaphase and metaphase. (b) P-S92-HP1α (green) and INCENP (red) colocalize at the centromere at metaphase. (c) The close proximity of P-S92-HP1α (green) and CENPA (red) signals was evident at metaphase. Scale bars = 10 μm.

other modifications previously described [39] to give rise to these different localization patterns for HP1α. To complement these observations, we performed proximity ligation assays (PLA) to detect *in situ* endogenous protein interactions between P-S92-HP 1α and AURKB or INCENP (Figure 2(f,g); Supplementary Figure 4A, 4B). PLA signals of P-S92-HP1α +AURKB complexes were significantly reduced

Table 1. HP1α interacts with critical kinetochore and microtubule network proteins during mitosis. Immunoprecipitation of HP1α from mitotic HeLa cells with subsequent mass spectrometry analysis identified 867 proteins that interact with HP1α during mitosis. HP1α/IgG specifies total unique peptide counts obtained with the HP1α antibody normalized to counts obtained with IgG. The table shows centromere and kinetochore components relevant to this study.

Protein Symbol	Protein Name	HP1α/IgG
CENPF	Centromere protein F	40
POGZ	Pogo transposable element with ZNF domain	35
NSL1	Kinetochore-associated protein NSL1 homolog	26
DSN1	Kinetochore-associated protein DSN1 homolog	11
NDC80	Kinetochore protein NDC80 homolog	9
SGOL1	Shugoshin-like 1	6
HP1α (CBX5)	Chromobox protein homolog 5	5
HP1γ (CBX3)	Chromobox protein homolog 3	4
INCENP	Inner centromere protein	4
BUB1	Mitotic checkpoint serine/threonine-protein kinase	4

in +hesperadin cells (0.28 ± 0.04 signals per cell +hesperadin compared to 2.67 ± 0.07 signals per cell for control cells -hesperadin, $p < 0.0001$). Similarly, PLA signals of P-S92-HP1α +INCENP complexes were significantly reduced in + hesperadin cells (1.29 ± 0.16 signals per cell +hesperadin as compared to 5.82 ± 0.17 signals per cells for control cells-hesperadin, $p < 0.0001$). In addition to pharmacological inhibition of Aurora B kinase activity, we reduced levels of AURKB through siRNA, which resulted in disruption of P-S92-HP1α localization patterns (Figure 3(a,e); Supplementary Figure 5A). P-S92-HP1α lost its colocalization with AURKB in siAURKB cells (0 ± 0 MOC compared to 0.70 ± 0.08 MOC in siCTRL, $p < 0.001$). Colocalization with INCENP revealed similar results (Figure 3(c,d)) (0 ± 0 MOC in siAURKB cells compared to 0.91 ± 0.03 MOC in siCTRL cells, $p < 0.0001$). As expected, PLA signals of P-S92-HP1α/AURKB complexes were lost in siAURKB cells (Figure 3(f); Supplementary Figure 6A) (0.33 ± 0.06 signals per cell compared to 3.0 ± 0.15 signals per cell for siCTRL cells, $p < 0.0001$). PLA signals of P-S92-HP1α/INCENP complexes were significantly reduced in siAURKB cells (Figure 3(g); Supplementary Figure 6B) (1.21 ± 0.12 signals per cell compared to compared to 5.91 ± 0.21 signals per cell for siCTRL cells, $p < 0.0001$). The concentric foci formed by INCENP at the centromere were lost with the reduction of AURKB levels (Figure 3(c)). Western blot analysis confirmed knockdown of AURKB and a reduction in P-S92-HP1α relative to total HP1α levels (Figure 3(e); Supplementary Figure 5A, 5B). In summary, these data reveal that the pool of P-S92-HP 1α that localizes to centromeric heterochromatin during mitosis requires the enzymatic activity of AURKB. Considering that many proteins located at the centromere-kinetochore participate in the regulation of chromosomal stability, our data raises the possibility that HP1α is involved in this phenomenon. Thus, subsequent experiments were aimed at testing the validity of this idea using genetic tools.

Genetic inactivation of HP1α results in mitotic and chromosomal aberrations

To evaluate the role of HP1α in chromosomal stability during mitosis, we used *Cbx5* (*Hp1α*) fl/fl MEFs carrying a tamoxifen-inducible form of Cre-recombinase. MEFs were serum-starved to arrest growth for 24 hr, and then the tamoxifen derivative, 4-hydroxytamoxifen (4′-OHT) was added for 48hr to initiate Cre-mediated recombination. Subsequently, cells were returned to complete growth media without 4′-OHT (designated 0hr). Control MEFs, CAGGCre-ER negative, underwent the same protocol (Figure 4(a)). Protein reduction was confirmed by immunofluorescence and Western blot (Figure 4(b,c); Supplementary Figure 7A, 7B). Fluorescent in situ hybridization (FISH) with a pan-centromeric probe on mitotic chromosome spreads demonstrated increased chromosomal breakage and fragmentation patterns induced upon depletion of *Hp1α* in primary MEFs (Figure 4(d)). Control primary MEFs (*Cbx5* +/+) did not show any of these described effects. Noteworthy, however, *Hp1α* deletion in MEFs (*Cbx5* -/-) resulted in increases in mitotic

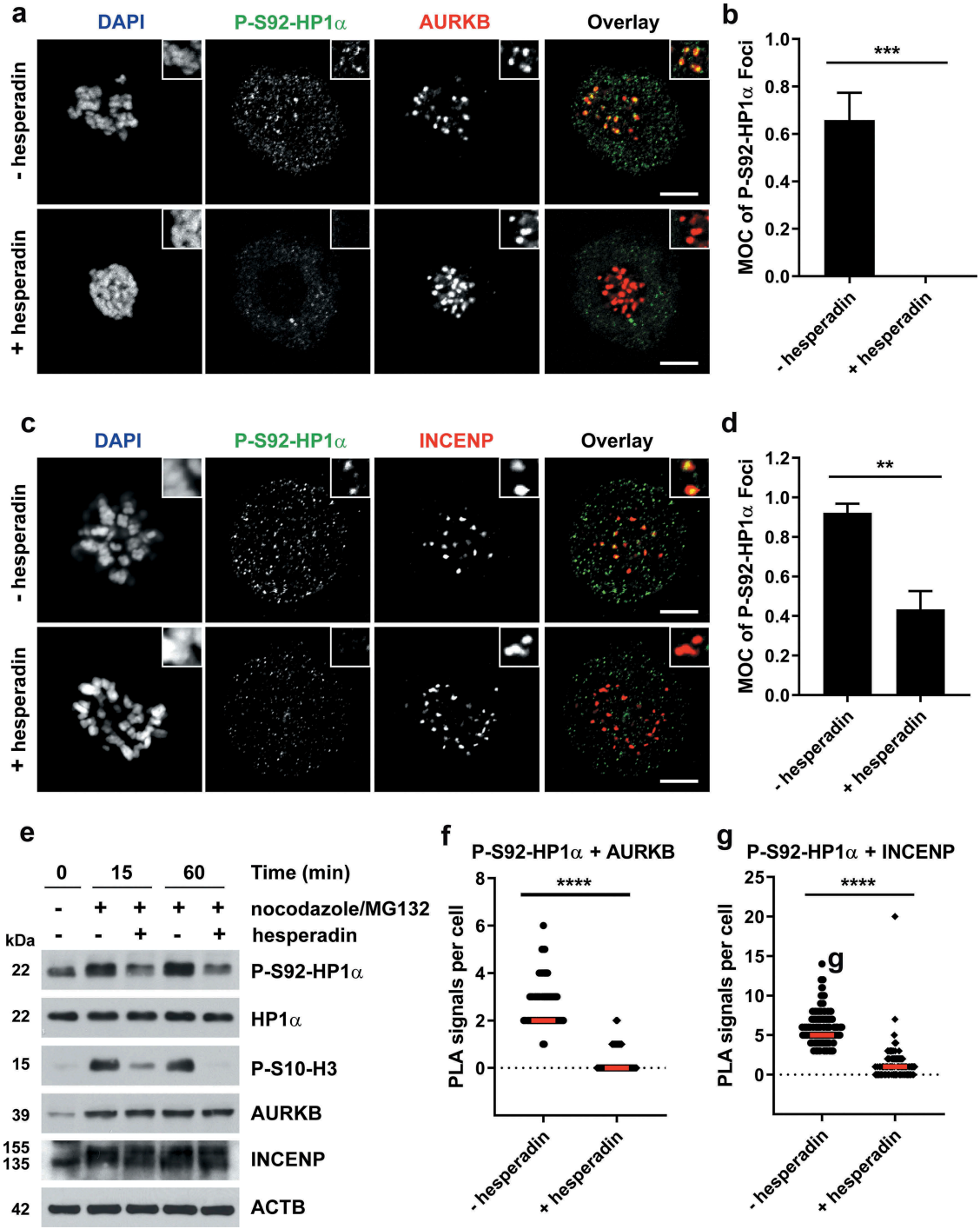

Figure 2. Inhibition of Aurora Kinase B activity with hesperadin perturbs phosphorylated HP1α centromere localization. (a) Immunofluorescence of P-S92-HP1α and AURKB (Aurora Kinase B) colocalization at the centromere upon pharmacological inhibition of AURKB with hesperadin for 1 hr in HeLa cells arrested in mitosis. Scale bars = 10 μm. (b) Manders overlap coefficient (MOC) of P-S92-HP1α and AURKB colocalization in total 150 cells in three independent experiments. (c) Immunofluorescence of P-S92-HP1α and INCENP (Inner centromere protein) colocalization at the centromere in identical conditions to (a). Scale bars = 10 μm. (d) Manders overlap coefficient of P-S92-HP1α and INCENP colocalization in total 150 cells in three independent experiments. (e) Western blot analysis of HP1α and P-S92-HP1α protein levels in response to pharmacological inhibition of AURKB at 0, 15, and 60min time intervals. Analysis of P-S10-H3 (phosphorylation of histone 3, serine 10) levels serves as a control for hesperadin/MG132 treatment efficacy, respectively. ACTB (β-actin) is the loading control. Full-length blots and quantification are presented in Supplementary Figure 3A and 3B. (f) Quantification and distribution of the number of proximity ligation assay (PLA) signals per cell (a total of 150 cells were counted over three independent experiments) where P-S92-HP1α overlaps with AURKB. (g) PLA signals where P-S92-HP1α overlaps INCENP in conditions identical to (f). Red line indicates the median value. IF images for PLA are presented in Supplementary Figure 4A and 4B. Statistical significance was determined by Student's t-test. Mean±sd, **p < 0.01, ***p < 0.001, ****p < 0.0001.

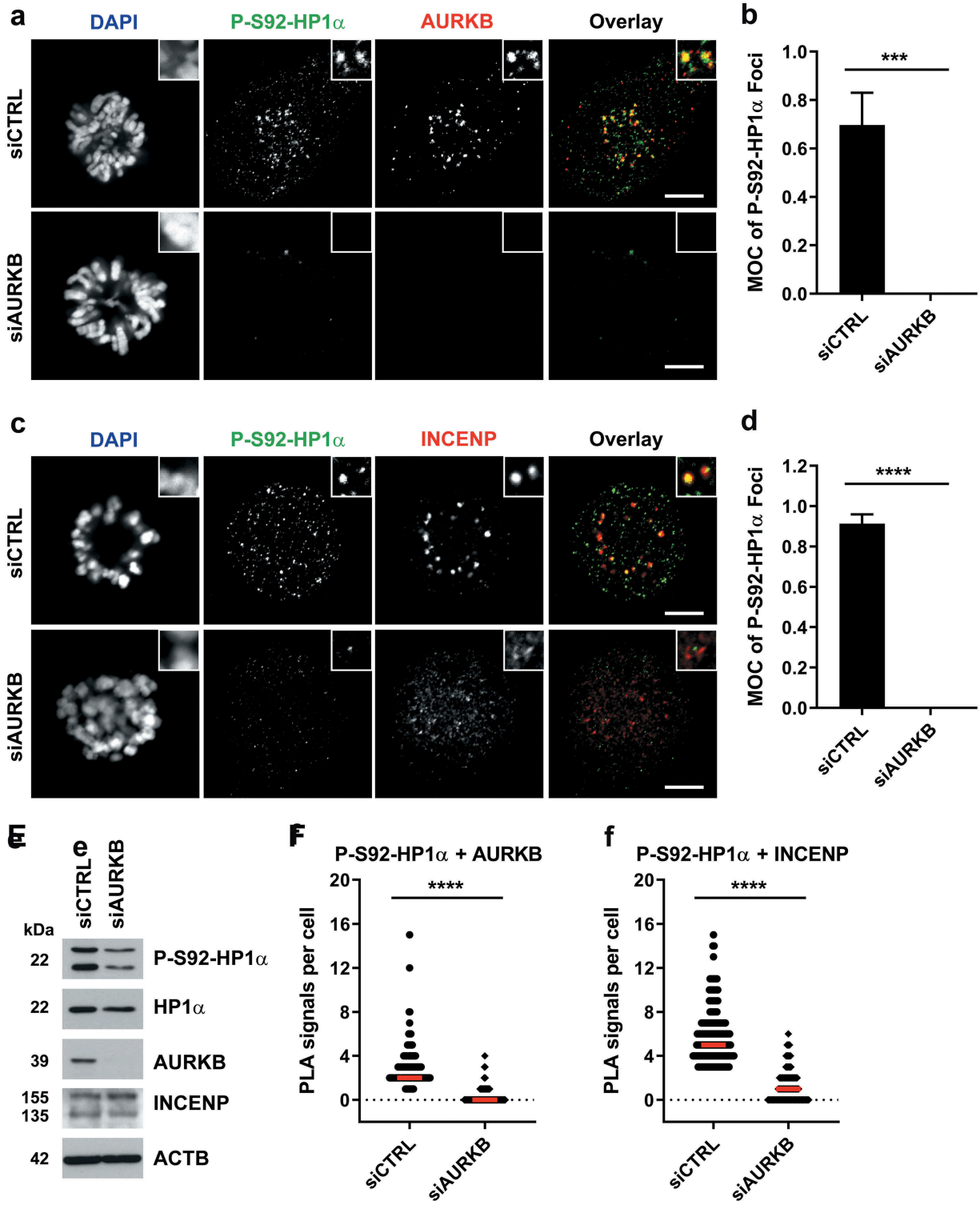

Figure 3. Knockdown of Aurora Kinase B protein abolishes centromere localization and reduces levels of phosphorylated HP1α. (a) Immunofluorescence of P-S92-HP1α and AURKB (Aurora Kinase B) colocalization at the centromere in metaphase HeLa cells exogenously expressing siRNA targeting AURKB. Scale bars = 10 µm. (b) Degree of colocalization of P-S92-HP1α and AURKB is expressed as a calculation of Manders overlap coefficient (MOC) in total 150 cells in three independent experiments. (c) Immunofluorescence of P-S92-HP1α and INCENP (Inner centromere protein) colocalization at the centromere in metaphase HeLa cells exogenously expressing siRNA targeting AURKB. (d) Manders overlap coefficient of P-S92-HP1α and INCENP colocalization in total 150 cells in three independent experiments. (e) AURKB knockdown is confirmed via Western blot with ACTB (β-actin) provided as the loading control. P-S92-HP1α levels are reduced. Full-length blots and quantification are presented in Supplementary Figure 5A and 5B. (f) Quantification and distribution of the number of proximity ligation assay (PLA) signals per cell (a total of 150 cells were counted over three independent experiments) where P-S92-HP1α overlaps with AURKB. (g) PLA signals where P-S92-HP1α overlaps INCENP in conditions identical to (f). Red line indicates the median value. IF images are presented in Supplementary Figure 6A and 6B. Statistical significance was determined by Student's t-test. Mean±sd, ***$p > 0.001$, ****$p < 0.0001$.

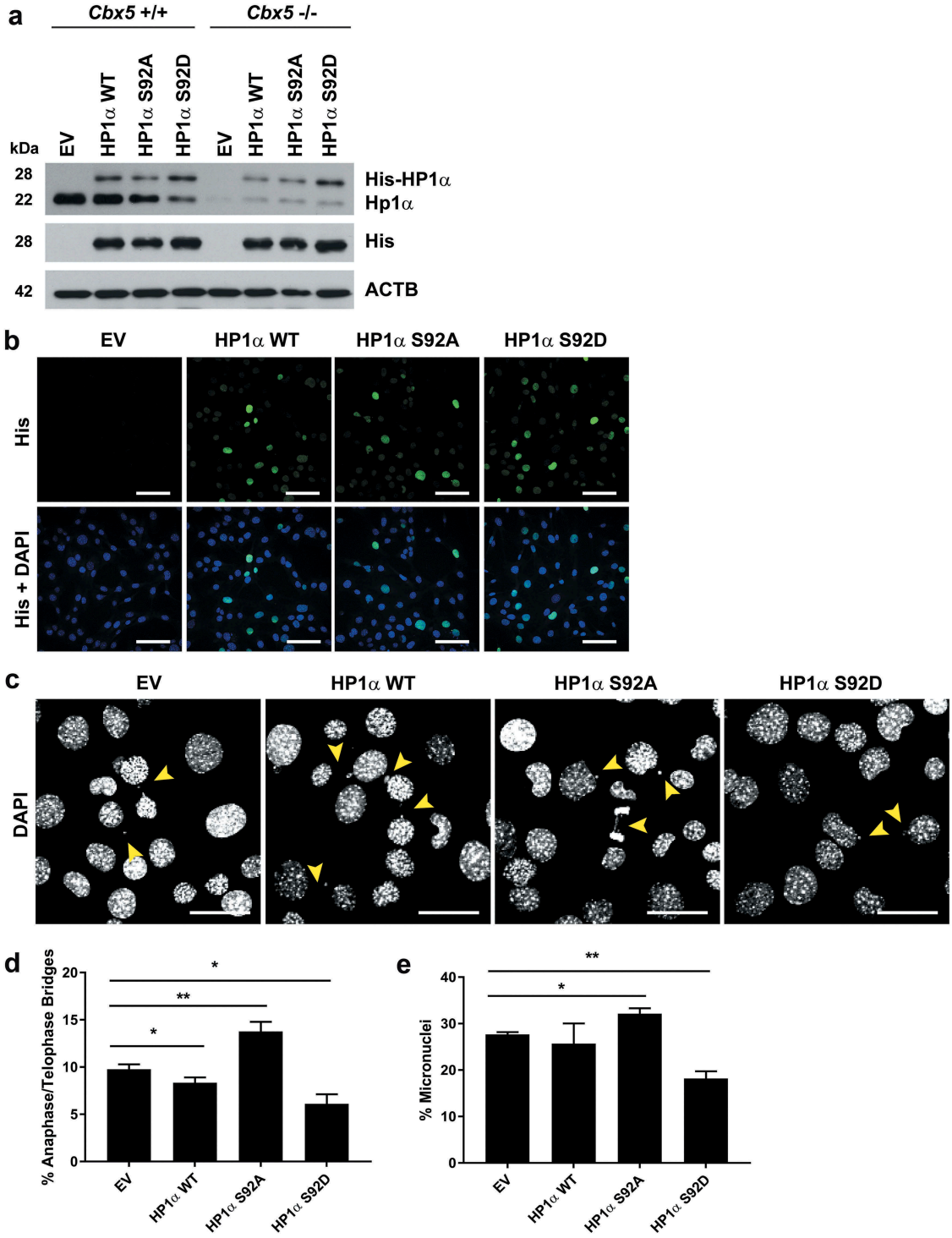

Figure 4. Loss of Hp1α (Cbx5) in normal mouse embryonic fibroblasts results in mitotic chromosomal abnormalities. (a) Schematic of 4′-hydroxy tamoxifen (4′-OHT) treatment protocol for achieving *Cbx5* knockout in primary and immortalized MEFs (*iCbx5*). Immunofluorescence (green, B) and western blot (c) confirmation of CBX5 knockout upon 4′-OHT-induced Cre recombination. Scale bars = 10 µm. Black and white images for IF are presented in Supplementary Figure 7A. Full-length blots are presented in Supplementary Figure 7B. ACTB (β-actin) is the loading control. (d) Fluorescent *in situ* hybridization (FISH) using a pan-centromeric probe shows chromosomal abnormalities (yellow arrowheads) induced upon *Cbx5* knockout in primary cells. (e) Quantification of chromosomal abnormalities in 60 chromosome spreads from three independent experiments. ROB (Robertsonian translocation). (f) Additional immunofluorescence of CBX5 (green) with DAPI staining of mitotic cells revealed an increase in anaphase/telophase chromatin bridges (yellow arrowheads). Quantification of chromatin bridges was completed with 1300 cells per condition in three independent experiments in the immortalized *Cbx5* (*iCbx5*) knockout cells. Scale bars = 10 µm. (g) An increased percentage of micronuclei (yellow arrowheads) were observed in the immortalized *Cbx5* (*iCbx5*) knockout cells. Quantification of micronuclei in 2600 cells per condition in three independent experiments. Scale bars = 20 µm. Black and white images for chromatin bridges and micronuclei are presented in Supplementary Figure 9A and 9B. Statistical significance was determined by Student's t-test. Mean±sd, *$p < 0.05$, **$p < 0.01$.

chromosomal abnormalities (Figure 4(e)). The significantly observed abnormalities included acentric fragments (53 ± 15 in knockout versus 4 ± 1 in control MEFs, $p < 0.05$), centromeric fragments (14 ± 2 in knockout versus 2 ± 0.3 in control MEFs, $p < 0.01$), and to a lesser extent, dicentric chromosomes (10 ± 2 in knockout versus 0.7 ± 0.3 in control MEFs, $p < 0.05$) and chromatid gaps (3 ± 0.6 in knockout versus 0.3 ± 0.3 in control MEFs, $p < 0.05$). Notably, a Robertsonian translocation (ROB) was found in 2.5% of the spreads analyzed. This abnormality is characterized by the rearrangement of the long arms of two different chromosomes that break at the centromere and then fuse to form a single large chromosome with a single centromere. Similar chromosomal abnormalities were identified by FISH in SV40 large T-immortalized *Cbx5* (*iCbx5*) MEFs upon 4′OHT-induced loss of *Hp1α* (Supplementary Figure 8A, 8B), further supporting the validity of our observations. Additional examination of these immortalized *Hp1α* knockout MEFs by immunofluorescence revealed the presence of mitotic abnormalities, including anaphase and telophase chromatin bridges (7.9 ± 0.6% in knockout compared to 1.5 ± 0.1% in control iMEFs, $p < 0.001$), and micronuclei formation (39.4 ± 8.2% in knockout compared to 13.5 ± 4.3% in control iMEFs, $p < 0.05$) as quantified in the total cell population (Figure 4(f,g); Supplementary Figure 9A, 9B). Thus, HP1α is required for proper chromosomal stability in MEFs.

Genetic complementation studies support a role for AURKB-mediated phosphorylation of HP1α in chromosomal stability

To determine the impact of S92 phosphorylation on this function of HP1α, we performed rescue experiments in our tamoxifen-inducible *Cbx5* (*Hp1α*) fl/fl MEFs, using adenovirus-mediated delivery of His-tagged, empty vector (EV) control, wild type human HP1α (WT), non-phosphorylatable (S92A), or phosphomimetic (S92D) HP1α proteins to evaluate the role of S92 phosphorylation in chromosomal stability. Western blot analysis (Figure 5(a); Supplemental Figure 10) in conjunction with immunofluorescence (Figure 5(b)) were used to control for endogenous HP1α deletion as well as exogenous HP1α expression. Higher magnification of cells (400X) clearly shows the presence of chromatin bridges and micronuclei that are reduced in the phosphomimetic (S92D) condition (Figure 5(c), yellow arrowheads). Quantification of anaphase and telophase chromatin bridges and cells with micronuclei (Figure 5(d,e)) showed that overexpression of wild type HP1α marginally decreased the number of chromosomal bridges (8.3 ± 0.6% as compared to 9.8 ± 0.5% in control EV cells, $p < 0.05$) and micronuclei (25.7 ± 4.4% as compared to 27.7 ± 0.5% in control EV cells, not significant). However, the phosphomimetic (S92D) mutant has a significant reduction in both chromatin bridges (6.1 ± 1.0% as compared to 9.8 ± 0.5% in control EV cells, $p < 0.05$) and micronuclei (18.2 ± 1.6% as compared to 27.7 ± 0.5% in control EV cells, $p < 0.01$). Similar results were seen in the immortalized MEFs (Supplementary Figure 11A, 11B). These results suggest that there was insufficient phosphorylation of the protein in cells overexpressing wild type HP1α, perhaps due to the absence of mitogenic stimuli, while the phosphomimetic mutant does not require phosphorylation, and thereby mitogenic stimuli, to rescue the chromosomal abnormalities. Conversely, overexpression of the non-phosphorylatable (S92A) mutant increased chromosomal bridges (13.8 ± 1.0% as compared to 9.8 ± 0.5% in control EV cells, $p < 0.01$) and micronuclei (32.2 ± 1.2% as compared to 27.7 ± 0.5% in control EV cells, $p < 0.05$) compared to the wild type protein (Figure 5(d,e)). Therefore, we conclude that AURKB-mediated phosphorylation at S92 of HP1α is necessary to maintain proper chromosome stability during mitosis.

Discussion

The current study further explores the role of HP1 proteins as part of the molecular machinery that mediates mitotic signals. The majority of our observations, reported here, indicate that HP1α, upon phosphorylation by Aurora Kinase B, localizes to mitotic centromere-kinetochore domains, where it co-localizes not only with this mitotic kinase but also with INCENP, which are both known to participate in the maintenance of

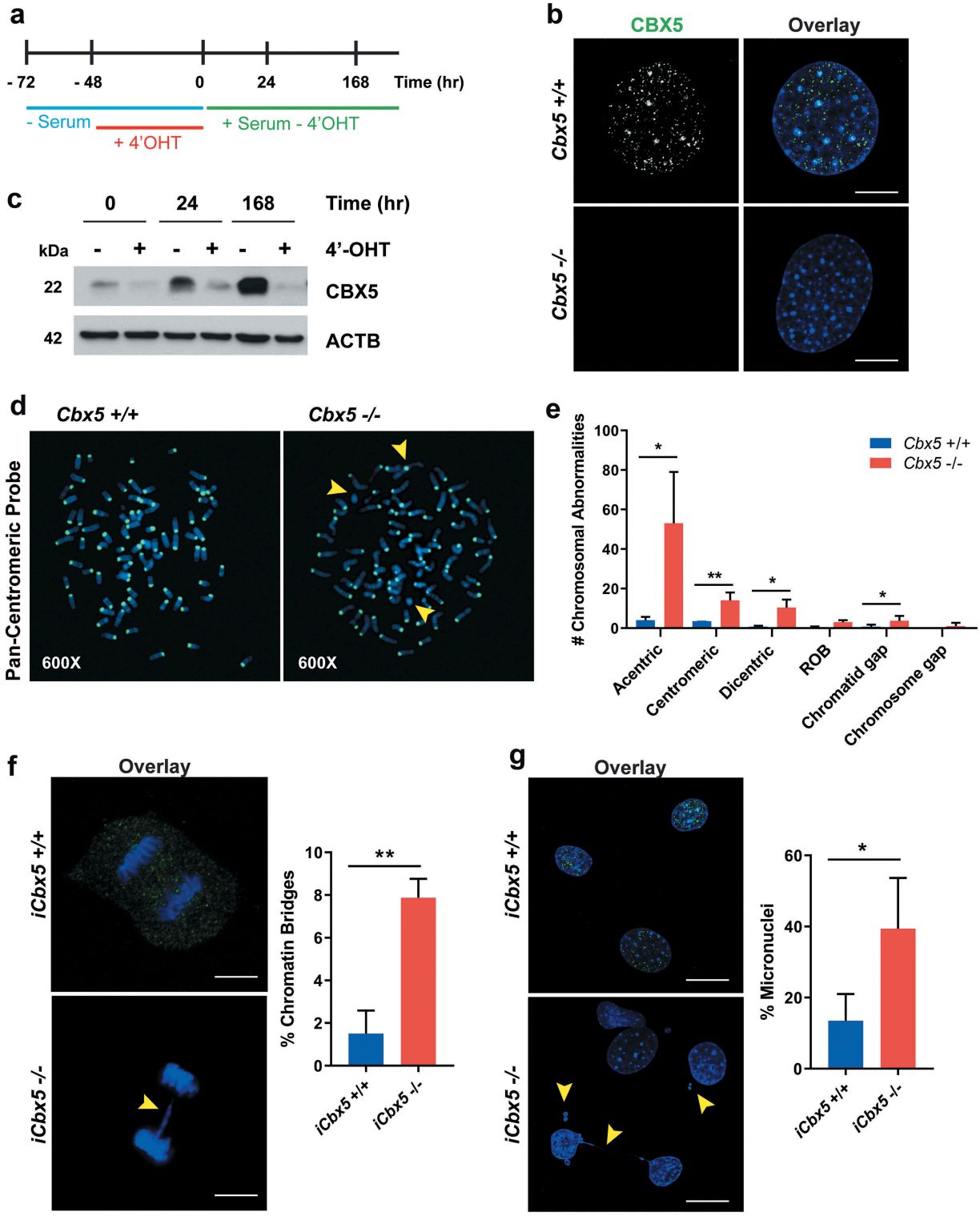

Figure 5. Restoration of HP1α in MEFs rescues mitotic chromosomal abnormalities in a phosphorylation-dependent manner. Rescue of the chromosomal instability phenotypes by reintroduction of empty vector (EV), His-tagged wild type (WT), non-phosphorylatable (S92A), or phosphomimetic (S92D) HP1α into *Cbx5* knockout MEFs via adenoviral transduction. (a) Western blot using anti-His antibody confirms expression of exogenous of HP1α proteins, while probing endogenous Hp1α shows reduction with *Cbx5* knockout. ACTB (β-actin) is the loading control. Full-length blots are presented in Supplementary Figure 10. (b) Immunofluorescence using anti-His antibody (green) confirms expression of exogenous of HP1α proteins. Scale bars = 110 µm. (c) Black and white images of DAPI stained cells with mitotic chromosomal abnormalities, chromatin bridges and micronuclei (yellow arrowheads). Scale bars = 30 µm. (d) Quantification of anaphase/telophase chromatin bridges and (e) micronuclei. Error bars represent s.d. of three independent experiments. Statistical significance was determined by Student's t-test. Mean±sd, *p < 0.05, **p < 0.01.

chromosomal stability. We confirm this localization and its dependence on active AURKB by indirect immunofluorescence and proximity ligation assays (PLA) using both pharmacological and siRNA approaches. Similar results observed with both hesperadin treatment and siRNA-mediated knockdown of AURKB, combined with consistent levels of AURKB protein upon hesperadin treatment (Figure 2(a,e)), strongly suggest that AURKB effects on HP1α function are a result of its kinase activity rather than protein levels of this mitotic kinase. While the phosphorylated form of HP1α localizes in close proximity to the inner kinetochore protein CENPA, the signals do not overlap, indicating that P-S92-HP1α is located within centromeric heterochromatin. More importantly, through using genetic approaches and assays for mitotic and chromosomal aberrations, we show that deletion of HP1α leads to abnormalities in these processes, which are rescued by the expression of a phosphomimetic S92D HP1α. Thus, this study of HP1α contributes to a better understanding of mitotic cell division and chromosomal stability, in normal development and diseases, such as cancer.

We found that phosphorylation of HP1α at S92 begins at prophase and becomes dissociated from chromosomes to localize to centromere-kinetochore domains. Thus, this protein can serve as a marker for both, mitosis and centromeres-kinetochores. We believe that, since these structures must form in a reproducible manner with each cell division, HP1α phosphorylated by AURKB serves as part of the previously described "HP1 subcode" that assigns particular functions to post-translationally modified reader proteins in a similar manner to histones [40]. For instance, P-S83-HP1γ, which we have shown to regulate mitotic functions downstream of Aurora A [27], serves as a marker of senescent cells [41]. This subcode is a conceptual framework for better understanding and classifying the function of these reader proteins at both the molecular and cellular levels. Interestingly, during our experiments, we noted that a non-chromatin-associated, cytoplasmic pool of P-S92-HP1α, was not affected by AURKB inhibition. This finding suggests the existence of mechanisms that render this non-chromatin-bound HP1α pool amenable to be phosphorylated at S92 kinases other than AURKB for phosphorylation. The conformation of the protein when released from chromatin may expose distinct recognition sites or post-translational modifications at other residues, which may influence kinase recruitment to offer specificity to distinguish unique pools of HP1α. The function of this non-chromatin-associated cytoplasmic P-S92-HP 1α would be an intriguing avenue for future studies to expand this subcode even further.

Recent studies identified AURKB as the main kinase responsible for phosphorylation of S92-HP 1α during mitosis [24]. In addition, Abe, et al. established HP1α as a component of the CPC required for optimal Aurora B kinase activity at the centromere-kinetochore [18]. Another study, utilizing a centromere-tethered HP1α, implicated the protein as the driver of CPC recruitment to the centromeres in G2 prior to its release at the beginning of mitosis [42]. These investigations increase our understanding of how HP1α is regulated throughout the cell cycle. The current study uses immunofluorescence in combination with pharmacological and genetic inhibition to extend this knowledge by showing that AURKB-mediated phosphorylation of this HP1α results in its localization to centromeric heterochromatin. Additionally, using genetic deletion of HP1α along with genetic complementation studies, we show that phosphorylation at S92 of HP1α appears to protect cells against mitotic and chromosomal aberrations. Thus, these results further highlight the importance of such post-translational modifications in HP1-mediated cell-cycle regulated functions, including senescence and chromosomal stability.

Author's Contributions

GL and RU generated the main idea of the work and developed the study design, both conceptually and methodologically. MW, AM, TC, PG, and DK made significant contributions to the acquisition of data. EK, MZ and JI provided expertise for analysis and interpretation of data. MW, AM, RU and GL wrote the manuscript from first draft to completion. All authors read, made substantial comments, suggested appropriate modifications and corrections, and approved the final manuscript.

Disclosure statement

No potential conflict of interest was reported by the authors.

Funding

This work was supported by National Institutes of Health Grants R01 CA178627 (to G.L.) and R01 DK52913 (to R.U.).

ORCID

Angela J. Mathison http://orcid.org/0000-0002-6763-2710
Michael T. Zimmermann http://orcid.org/0000-0001-7073-0525
Juan Iovanna http://orcid.org/0000-0003-1822-2237
Gwen A. Lomberk http://orcid.org/0000-0001-5463-789X

References

[1] Eissenberg JC, James TC, Foster-Hartnett DM, et al. Mutation in a heterochromatin-specific chromosomal protein is associated with suppression of position-effect variegation in Drosophila melanogaster. Proc Natl Acad Sci U S A. 1990;87:9923–9927.
[2] James TC, Elgin SC. Identification of a nonhistone chromosomal protein associated with heterochromatin in Drosophila melanogaster and its gene. Mol Cell Biol. 1986;6:3862–3872.
[3] Eissenberg JC, Elgin SCR. The HP1 protein family: getting a grip on chromatin. Curr Opin Genet Dev. 2000;10:204–210.
[4] Lomberk G, Wallrath L, Urrutia R. The Heterochromatin Protein 1 family. Genome Biol. 2006;7:228.
[5] Stewart MD, Li J, Wong J. Relationship between histone H3 lysine 9 methylation, transcription repression, and heterochromatin protein 1 recruitment. Mol Cell Biol. 2005;25:2525–2538.
[6] Wolfgang Fischle BST, Dormann HL, Ueberheide BM, et al. Regulation of HP1–chromatin binding by histone H3 methylation and phosphorylation. Nature. 2005;438:1116–1122.
[7] Eissenberg JC, Elgin SCR. HP1a: a structural chromosomal protein regulating transcription. Trends Genet. 2014;30:103–110.
[8] Nestorov P, Tardat M, Peters AHFM. Current topics in developmental biology: Epigenetics and development, Vol. 104, ed Edith Heard. San Diego (CA): Academic Press; 2013. p. 243–291.
[9] Dinant C, Luijsterburg MS. The emerging role of HP1 in the DNA damage response. Mol Cell Biol. 2009;29:6335–6340.
[10] Prendergast JMGHAL. Mitotic mysteries: the case of HP1. Dev Cell. 2016;36:477–478.
[11] So Hee K, Jerry LW. The heterochromatin protein 1 (HP1) family: put away a bias toward HP1. Mol Cells. 2008;26:217–227.
[12] Wu W, Togashi Y, Johmura Y, et al. HP1 regulates the localization of FANCJ at sites of DNA double-strand breaks. Cancer Sci. 2016;107:1406–1415.
[13] Ainsztein AM, Kandels-Lewis SE, Mackay AM, et al. INCENP centromere and spindle targeting: identification of essential conserved motifs and involvement of heterochromatin protein HP1. J Cell Biol. 1998;143:1763–1774.
[14] Carmena M, Platani PX, Salloum Z, et al. The chromosomal passenger complex activates polo kinase at centromeres. PLoS Biol. 2012;10:e1001250.
[15] Mar Carmena MW, Funabiki H, Earnshaw WC. The chromosomal passenger complex (CPC): from easy rider to the godfather of mitosis. Nat Rev Mol Cell Biol. 2012;13:789–803.
[16] Gassmann R, Carvalho A, Henzing AJ, et al. Borealin: a novel chromosomal passenger required for stability of the bipolar mitotic spindle. J Cell Biol. 2004;166:179–191.
[17] Liu X, Song Z, Huo Y, et al. Chromatin protein HP1α interacts with the mitotic regulator borealin protein and specifies the centromere localization of the chromosomal passenger complex. J Biol Chem. 2014;289:20638–20649.
[18] Abe Y, Sako K, Takagaki K, et al. HP1-assisted AURORA B kinase activity prevents chromosome segregation errors. Dev Cell. 2016;36:487–497.
[19] Kang J, Chaudhary J, Dong H, et al. Mitotic centromeric targeting of HP1 and its binding to Sgo1 are dispensable for sister-chromatid cohesion in human cells. Mol Biol Cell. 2011;22:1181–1190.
[20] Canzio D, Chang EY, Shankar S, et al. Chromodomain-mediated oligomerization of HP1 suggests a nucleosome-bridging mechanism for heterochromatin assembly. Mol Cell. 2011;41:67–81.
[21] Chu L, Huo Y, Liu X, et al. The spatiotemporal dynamics of chromatin protein HP1α is essential for accurate chromosome segregation during cell division. J Biol Chem. 2014;289:26249–26262.
[22] Chakraborty A, Prasanth KV, Prasanth SG. Dynamic phosphorylation of HP1α regulates mitotic progression in human cells. Nat Commun. 2014;5:3445.
[23] Hayakawa T, Haraguchi T, Masumoto H, et al. Cell cycle behavior of human HP1 subtypes: distinct molecular domains of HP1 are required for their centromeric localization during interphase and metaphase. J Cell Sci. 2003;116:3327.
[24] Nishibuchi G, Machida S, Nakagawa R, et al. Mitotic phosphorylation of HP1alpha regulates its cell cycle-dependent chromatin binding. J Biochem. 2018. DOI:10.1093/jb/mvy117.
[25] Ma HT, Poon RYC. Cell cycle synchronization: methods and protocols (ed Gaspar Banfalvi). Humana Press; 2011. p. 151–161.
[26] Fischle W, Tseng BS, Dormann HL, et al. Regulation of HP1–chromatin binding by histone H3 methylation and phosphorylation. Nature. 2005;438:1116.
[27] Grzenda A, Leonard P, Seo S, et al. Functional impact of Aurora A-mediated phosphorylation of HP1γ at serine 83 during cell cycle progression. Epigenetics Chromatin. 2013;6:21.

[28] Schneider CA, Rasband WS, Eliceiri KW. NIH Image to ImageJ: 25 years of image analysis. Nat Methods. 2012;9:671.
[29] Costes SV, Daelemans D, Cho EH, et al. Automatic and quantitative measurement of protein-protein colocalization in live cells. Biophys J. 2004;86:3993–4003.
[30] Dunn KW, Kamocka MM, McDonald JH. A practical guide to evaluating colocalization in biological microscopy. Am J Physiol Cell Physiol. 2011;300:C723–C742.
[31] Skoufias DA, DeBonis S, Saoudi Y, et al. S-trityl-L-cysteine is a reversible, tight binding inhibitor of the human kinesin Eg5 that specifically blocks mitotic progression. J Biol Chem. 2006;281:17559–17569.
[32] van Leuken R, Clijsters L, van Zon W, et al. Polo-like kinase-1 controls Aurora A destruction by activating APC/C-Cdh1. PloS One. 2009;4:e5282.
[33] Durkin ME, Qian X, Popescu NC, et al. Isolation of mouse embryo fibroblasts. Bio-Protocol. 2013;3:e908.
[34] Mathison A, Liebl A, Bharucha J, et al. Pancreatic stellate cell models for transcriptional studies of desmoplasia-associated genes. Pancreatology. 2010;10:505–516.
[35] Black BE, Bassett EA. The histone variant CENP-A and centromere specification. Curr Opin Cell Biol. 2008;20:91–100.
[36] Black BE, Brock MA, Bedard S, et al. An epigenetic mark generated by the incorporation of CENP-A into centromeric nucleosomes. Proc Natl Acad Sci U S A. 2007;104:5008–5013.
[37] Sekulic N, Bassett EA, Rogers DJ, et al. The structure of (CENP-A/H4)(2) reveals physical features that mark centromeres. Nature. 2010;467:347–351.
[38] Maiato H, DeLuca J, Salmon ED, et al. The dynamic kinetochore-microtubule interface. J Cell Sci. 2004;117:5461–5477.
[39] LeRoy G, Weston JT, Zee BM, et al. Heterochromatin protein 1 is extensively decorated with histone code-like post-translational modifications. Mol Cell Proteomics. 2009;8:2432–2442.
[40] Lomberk G, Bensi D, Fernandez-Zapico ME, et al. Evidence for the existence of an HP1-mediated subcode within the histone code. Nat Cell Biol. 2006;8:407.
[41] Zhang R, Chen W, Adams PD. Molecular dissection of formation of senescence-associated heterochromatin foci. Mol Cell Biol. 2007;27:2343–2358.
[42] Ruppert JG, Samejima K, Platani M, et al. HP1α targets the chromosomal passenger complex for activation at heterochromatin before mitotic entry. Embo J. 2018;37:e97677.